A Combined Anomaly Detection and Failure Prognosis Approach for Estimation of Remaining Useful Life in Energy Storage Devices

Marcos E. Orchard[1], Liang Tang[2], and George Vachtsevanos[3]

[1]*Electrical Engineering Department, Universidad de Chile, Santiago 8370451, Chile*
morchard@ing.uchile.cl

[2]*Impact Technologies, LLC, Rochester, NY 14623, USA*
liang.tang@impact-tek.com

[3]*School of Electrical and Computer Engineering, Georgia Institute of Technology, Atlanta, GA 30332, USA*
[2]*Impact Technologies, LLC, Rochester, NY 14623, USA*
gjv@ece.gatech.edu

ABSTRACT

Failure prognosis and uncertainty representation in long-term predictions are topics of paramount importance when trying to ensure safety of the operation of any system. In this sense, the use of particle filter (PF) algorithms -in combination with outer feedback correction loops- has contributed significantly to the development of a robust framework for online estimation of the remaining useful equipment life. This paper explores the advantages of using a combination of PF-based anomaly detection and prognosis approaches to isolate rare events that may affect the understanding about how the fault condition evolves in time. The performance of this framework is thoroughly compared using a set of ad hoc metrics. Actual data illustrating aging of an energy storage device (specifically battery state-of-health (SOH) measurements [A-hr]) are used to test the proposed framework.

1. INTRODUCTION

Particle-filtering (PF) based prognostic algorithms (Orchard, 2009; Orchard and Vachtsevanos, 2009; Orchard *et al*., 2009) have been established as the de facto state of the art in failure prognosis. PF algorithms allow avoiding the assumption of Gaussian (or log-normal) probability density function (pdf) in nonlinear processes, with unknown model parameters, and simultaneously help to consider non-uniform probabilities of failure for particular regions of the state domain. Particularly, the authors in (Orchard *et al.* 2008) have proposed a mathematically rigorous method (based on PF, function kernels, and outer correction loops) to represent and manage uncertainty in long-term predictions. However, there are still unsolved issues regarding the proper representation for the probability of rare events and highly non-monotonic phenomena, since these events are associated to particles located at the tails of the predicted probability density functions.

This paper presents a solution for this problem that is based on a combination of a PF-based anomaly detection modules (which are in charge of detecting rare events within the evolution of the fault condition under analysis) and PF-prognostic schemes to estimate the remaining useful life of a piece of equipment. The paper is structured as follows: Section 2 introduces the basics of particle filtering (PF) and its application to the field of anomaly detection and failure prognostics. Section 3 presents a combined framework using actual failure data measuring battery state-of-health (SOH, [A hr]), where it is of interest to detect capacity regeneration phenomena in an online fashion. Section 4 utilizes performance metrics to assess prognostic results and evaluates the proposed scheme, when compared to the classic PF prognosis framework (Orchard, 2009; Orchard and Vachtsevanos, 2009; Vachtsevanos *et al.*, 2006). Section 5 states the main conclusions.

2. PARTICLE FILTERING, ANOMALY DETECTION AND FAILURE PROGNOSIS

Nonlinear filtering is defined as the process of using noisy observation data to estimate at least the first two moments of a state vector governed by a dynamic nonlinear, non-Gaussian state-space model. From a Bayesian standpoint, a nonlinear filtering procedure intends to generate an estimate of the posterior probability density function $p(x_t \mid y_{1:t})$ for the state, based on the set of received measurements. Particle Filtering (PF) is an algorithm that intends to solve this estimation problem by efficiently selecting a set of *N* particles $\{x^{(i)}\}_{i=1\cdots N}$ and weights $\{w_t^{(i)}\}_{i=1\cdots N}$, such that the

state pdf may be approximated (Doucet, 1998; Doucet *et al.*, 2001; Andrieu *et al*, 2001; Arulampalam *et al.*, 2002) by:

$$\begin{aligned} \tilde{\pi}_t^N(x_t) &= \sum_{i=1}^{N} w_t^{(i)} \delta(x_t - x_t^{(i)}) \\ w(x_{0:t}) &= \frac{\pi_t(x_{0:t})}{q_t(x_{0:t})} \propto \frac{p(y_t \mid x_t)\, p(x_t \mid x_{0:t-1})}{q_t(x_t \mid x_{0:t-1})} \end{aligned} \quad , \tag{1}$$

where $q_t(x_{0:t})$ is referred to as the importance sampling density function (Arulampalam *et al.*, 2002; Doucet *et al.*, 2001). The choice of this importance density function is critical for the performance of the particle filter scheme. In the particular case of nonlinear state estimation, the value of the particle weights $w_{0:t}^{(i)}$ is computed by setting the importance density function equal to the *a priori* pdf for the state, i.e., $q_t(x_{0:t} \mid x_{0:t-1}) = p(x_t \mid x_{t-1})$ (Arulampalam *et al.*, 2002). Although this choice of importance density is appropriate for estimating the most likely probability distribution according to a particular set of measurement data, it does not offer a good estimate of the probability of events associated to high-risk conditions with low likelihood. This paper explores the possibility of using a PF-based detection scheme to isolate those types of events.

2.1 PF-based Anomaly Detection

A PF-based anomaly detection procedure (Orchard and Vachtsevanos, 2009; Verma *et al.*, 2004) aims at the identification of abnormal conditions in the evolution of the system dynamics, under assumptions of non-Gaussian noise structures and nonlinearities in process dynamic models, using a reduced particle population to represent the state pdf. The method also allows fusing and utilizing information present in a feature vector (measurements) to determine not only the operating condition (mode) of a system, but also the causes for deviations from desired behavioral patterns. This compromise between model-based and data-driven techniques is accomplished by the use of a PF-based module built upon the nonlinear dynamic state model (2):

$$\begin{cases} x_d(t+1) = f_b\left(x_d(t) + n(t)\right) \\ x_c(t+1) = f_t(x_d(t), x_c(t), \omega(t)) \\ \text{Features}(t) = h_t(x_d(t), x_c(t), v(t)) \end{cases} , \tag{2}$$

where f_b, f_t and h_t are non-linear mappings, $x_d(t)$ is a collection of Boolean states associated with the presence of a particular operating condition in the system (normal operation, fault type #1, #2), $x_c(t)$ is a set of continuous-valued states that describe the evolution of the system given those operating conditions, $\omega(t)$ and $v(t)$ are non-Gaussian distributions that characterize the process and feature noise signals respectively. Since the noise signal $n(t)$ is a measure of uncertainty associated with Boolean states, it is recommendable to define its probability density through a random variable with bounded domain. For simplicity, $n(t)$ may be assumed to be zero-mean i.i.d. uniform white noise.

A particle filtering approach based on model (2) allows statistical characterization of both Boolean and continuous-valued states, as new feature data are received. As a result, at any given instant of time, this framework provides an estimate of the probability masses associated with each fault mode, as well as a pdf estimate for meaningful physical variables in the system. Once this information is available within the anomaly detection module, it is conveniently processed to generate proper fault alarms and to inform about the statistical confidence of the detection routine.

Furthermore, pdf estimates for the system continuous-valued states (computed at the moment of fault detection) may be also used as initial conditions in failure prognostic routines, giving an excellent insight about the inherent uncertainty in the prediction problem. As a result, a swift transition between the two modules (anomaly detection and prognosis) may be performed, and moreover, reliable prognosis can be achieved within a few cycles of operation after the fault is declared.

2.2 PF-based Failure Prognosis

Prognosis, and more generally, the generation of long-term predictions, is a problem that goes beyond the scope of filtering applications since it involves future time horizons. Hence, if PF-based algorithms are to be used for prognosis, a procedure is required that has the capability to project the current particle population into the future in the absence of new observations (Orchard, 2009; Orchard and Vachtsevanos, 2009).

Any prognosis scheme requires the existence of at least one feature providing a measure of the severity of the fault condition under analysis (fault dimension). If many features are available, they can in principle be combined to generate a single signal. In Therefore, it is possible to describe the evolution in time of the fault dimension through the nonlinear state equation (Orchard *et al.*, 2008):

$$\begin{cases} x_1(t+1) = x_1(t) + x_2(t) \cdot F(x(t), t, U) + \omega_1(t) \\ x_2(t+1) = x_2(t) + \omega_2(t) \\ y(t) = x_1(t) + v(t) \end{cases} , \tag{3}$$

where $x_1(t)$ is a state representing the fault dimension under analysis, $x_2(t)$ is a state associated with an unknown model parameter, U are external inputs to the system (load profile, etc.), $F(x(t), t, U)$ is a general time-varying nonlinear function, and $\omega_1(t)$, $\omega_2(t)$, $v(t)$ are white noises (not necessarily Gaussian). The nonlinear function $F(x(t), t, U)$ may represent a model, for example a model based on first principles, a neural network, or model based on fuzzy logic.

By using the aforementioned state equation to represent the evolution of the fault dimension in time, one can generate long term predictions using kernel functions to reconstruct the estimate of the state pdf in future time instants (Orchard *et al.*, 2008):

$$\hat{p}(x_{t+k} \mid \hat{x}_{1:t+k-1}) \approx \sum_{i=1}^{N} w_{t+k-1}^{(i)} K\left(x_{t+k} - E\left[x_{t+k}^{(i)} \mid \hat{x}_{t+k-1}^{(i)}\right]\right), \quad (4)$$

where $K(\cdot)$ is a kernel density function, which may correspond to the process noise pdf, a Gaussian kernel or a rescaled version of the Epanechnikov kernel.

The resulting predicted state pdf contains critical information about the evolution of the fault dimension over time. One way to represent that information is through the expression of statistics (expectations, 95% confidence intervals), either the End-of-Life (EOL) or the Remaining Useful Life (RUL) of the faulty system. A detailed procedure to obtain the RUL pdf from the predicted path of the state pdf is described and discussed in (Orchard, 2009; Patrick *et al.*, 2007; Zhang *et al.*, 2009). Essentially, the RUL pdf can be computed from the function of probability-of-failure at future time instants. This probability is calculated using both the long-term predictions and empirical knowledge about critical conditions for the system. This empirical knowledge is usually incorporated in the form of thresholds for main fault indicators (also referred to as the hazard zones).

In real applications, hazard zones are expected to be statistically determined on the basis of historical failure data, defining a critical pdf with lower and upper bounds for the fault indicator (H_{lb} and H_{ub}, respectively). Let the hazard zone specify the probability of failure for a fixed value of the fault indicator, and the weights $\left\{w_{t+k}^{(i)}\right\}_{i=1\cdots N}$ represent the predicted probability for the set of predicted paths, then the probability of failure at any future time instant (namely the RUL pdf) by applying the law of total probabilities, as shown in Eq. (5).

$$\hat{p}_{TTF}(t) = \sum_{i=1}^{N} \Pr\left(Failure \mid X = \hat{x}_t^{(i)}, H_{lb}, H_{ub}\right) \cdot w_t^{(i)} \quad (5)$$

Once the RUL pdf has been computed by combining the weights of predicted trajectories with the hazard zone specifications, prognosis confidence intervals, as well as the RUL expectation can be extracted.

3. A COMBINED ANOMALY DETECTION AND FAILURE PROGNOSIS APPROACH: CASE STUDY DEFINITION

An appropriate case study has been selected to demonstrate the efficacy of a scheme that includes a PF-based anomaly detection module working in combination with a PF-based prognostic algorithm. Consider the case of energy storage devices, particularly of Li-Ion batteries, where continuous switching between charge and discharge cycles may cause momentary increments in the battery SOH (capacity regeneration). These sudden increments directly affect RUL estimates in a classic PF-based prognostic scheme since the state pdf estimate has to be adjusted to according to new measurements (thus modifying long-term predictions), while the observed phenomenon typically disappears after a few cycles of operation. Particularly in the case of Li-Ion batteries, the regeneration phenomena can produce an unexpected short-term increment of the battery SOH of about 10% of the nominal capacity.

The analysis of the aforementioned phenomena will be done using data registering two different operational profiles (charge and discharge) at room temperature. On the one hand, charging is carried out in a constant current (CC) mode at 1.5[A] until the battery voltage reached 4.2[V] and then continued in a constant voltage mode until the charge current dropped to 20[mA]. On the other hand, discharge is carried out at a constant current (CC) level of 2[A] until the battery voltage fell to 2.5[V]. Impedance measurements provide insight into the internal battery parameters that change as aging progresses. Repeated charge and discharge cycles result in aging of the batteries. Impedance measurements were done through an electrochemical impedance spectroscopy (EIS) frequency sweep from 0.1[Hz] to 5[kHz]. The experiments were stopped when the batteries reached end-of-life (EOL) criteria, which was a 40% fade in rated capacity (from 2[A-hr] to 1.2[A-hr]). This dataset can be used both for the prediction of both remaining charge (for a given discharge cycle) and remaining useful life (RUL).

Two main operating conditions are thus distinguished: the *normal* condition reflects the fact that the battery SOH is slowly diminishing as a function of the number of charge/discharge cycles; while the *anomalous* condition indicates an abrupt increment in the battery SOH (regeneration phenomena). To detect the condition of interest, a PF-based anomaly detection module is implemented using nonlinear model (6), where $x_{d,1}$ and $x_{d,2}$ are Boolean states that indicate *normal* and *anomalous* conditions respectively, x_{c1} is the continuous-valued state that represents the battery SOH, β is a positive time-varying model parameter, x_{c2} is the added SOH because of the capacity regeneration phenomena, and where $\omega(t)$ and $v(t)$ have been selected as zero mean Gaussian noises for simplicity. The initial battery SOH in the data set used for this analysis is 2[A-hr.], which determines the initial condition of (6).

Besides detecting the regeneration condition, it is desired to obtain some measure of the statistical confidence of the alarm signal. For this reason, two outputs can be extracted from the anomaly detection module. The first output is the expectation of the Boolean state $x_{d,2}$, which constitutes an

estimate of the probability of regeneration. The second output is the statistical confidence needed to declare the condition via hypothesis testing (H_0: "no anomaly is being detected" vs. H_1: "capacity regeneration is being detected"). The latter output needs another pdf to be considered as the baseline. In this case, that pdf could be the filtering estimate of state x_{c1}.

$$\begin{cases} \begin{bmatrix} x_{d,1}(t+1) \\ x_{d,2}(t+1) \end{bmatrix} = f_b\left(\begin{bmatrix} x_{d,1}(t) \\ x_{d,2}(t) \end{bmatrix} + n(t) \right) \\ x_{c1}(t+1) = (1-\beta) x_{c1}(t) + \omega_1(t) \\ x_{c2}(t+1) = 0.95 x_{c2}(t) \cdot x_{d,2}(t) + 0.2 x_{d,1}(t) + \omega_2(t) \end{cases}$$

$$y(t) = x_{c1}(t) + x_{c2}(t) \cdot x_{d,2}(t) + v(t) \qquad (6)$$

$$f_b(x) = \begin{cases} \begin{bmatrix} 1 & 0 \end{bmatrix}^T \text{, if } \left\| x - \begin{bmatrix} 1 & 0 \end{bmatrix}^T \right\| \le \left\| x - \begin{bmatrix} 0 & 1 \end{bmatrix}^T \right\| \\ \begin{bmatrix} 0 & 1 \end{bmatrix}^T \text{, else} \end{cases}$$

$$\begin{bmatrix} x_{d,1}(0) & x_{d,2}(0) & x_{c1}(0) & x_{c2}(0) \end{bmatrix}^T = \begin{bmatrix} 1 & 0 & 2 & 0 \end{bmatrix}^T$$

Moreover, since this is a PF-based module, one way to generate an on-line indicator of statistical confidence for the detection procedure is to consider the sum of the weights of all particles i such that $x_c^{(i)}(T) \ge z_{1-\alpha,\mu,\sigma^2}$, where α is the desired test confidence and T is the detection time, which is essentially equivalent to an estimate of (1 – *type II error*), or equivalently the probability of detection. If additional information is required, it is possible to compute the value of the Fisher's Discriminant Ratio, as in (7).

$$F_{index}(T) = \frac{\left| \mu - \sum_{i=1}^{N} w_T^{(i)} \cdot x_c^{(i)}(T) \right|^2}{\left(\sigma^2 + \sum_{i=1}^{N} w_T^{(i)} \cdot \left(x_c^{(i)}(T) - \sum_{j=1}^{N} w_T^{(j)} \cdot x_c^{(j)}(T) \right)^2 \right)} \qquad (7)$$

It must be noted that, in this approach, no particular specification about the detection threshold has to be made prior to the actual experiment. Customer specifications are translated into acceptable margins for the *type I* and *II* errors in the detection routine. The algorithm itself will indicate when the *type II error* (false negatives) has decreased to the desired level.

Once the regeneration phenomena have been adequately isolated, it is the task of the PF-based prognosis framework to come up with a pdf estimate of the remaining useful life of the Li-Ion battery. For this purpose, instead of a physics-based model we will employ here a population-growth-based model (Patrick *et al.*, 2007; Orchard et al., 2008, Zhang *et al.*, 2009) that has been trained using online SOH measurements (fault dimension in [A-hr]), where $x_1(t)$ is a state representing the fault dimension, $x_2(t)$ is a state associated with an unknown model parameter, $x_3(t)$ is a state associated with the capacity regeneration phenomena, a, b, C and m are constants associated to the duration and intensity of the battery load cycle (external input U), and $0 \le \alpha \le 1$ is a parameter that characterizes the regeneration.

$$\begin{cases} x_1(t+1) = x_1(t) + C \cdot x_2(t) \cdot (a - b \cdot t + t^2)^m + \omega_1(t) \\ x_2(t+1) = x_2(t) + \omega_2(t) \\ x_3(t+1) = \alpha \cdot x_3(t) + \omega_3(t) \end{cases}, \qquad (8)$$

$$y(t) = x_1(t) + x_3(t) + v(t)$$

The objective of a prognostic routine applied to the system defined by (8), and particularly for the ones based on PF algorithms, is to estimate (preferably in an online fashion) the current battery SOH, isolating the effect of the regeneration phenomena, and to use that information to estimate the amount of cycles remaining until this quantity falls below the threshold of 1.2[A-hr].

The analysis will focus on the quality of the estimate for the state components x_1 and x_3, after each capacity regeneration phenomena and on the accuracy exhibited by the corresponding End-of-Life (EOL) pdf estimate. Performance comparison is done with respect to a classic (SIR) PF-based prognostic framework (Orchard *et al.*, 2009), given same initial conditions. It should be noted that the implementation chosen here considers a correction loop that simultaneously updates the variance of kernel associated to the white noise $\omega_2(t)$ according to the short-term prediction (Orchard, Tobar and Vachtsevanos, 2010).

The implementation of the aforementioned scheme has been performed using MATLAB® environment. A complete description of the results obtained, and a comparison with classic PF-based routines, follows in Section 4.

4. ASSESSMENT AND EVALUATION OF THE PROPOSED FRAMEWORK USING PERFORMANCE METRICS

Estimates obtained from a Particle Filtering algorithm are based on the realization of a stochastic process and measurement data. Assessment or comparison between different strategies should consider performance statistics rather than a performance assessment based on a single experiment or realization. For that reason, all results presented in this paper consider the statistical mean of 30 realizations for the particle filter algorithm and a single measurement data set (no major differences were found when considering more realizations).

In addition, the assessment and evaluation of prognostic algorithms require appropriate performance metrics capable of incorporating concepts such as "accuracy" and "precision" of the RUL pdf estimate (Vachtsevanos *et al.*, 2006). "Accuracy" is defined as the difference between the actual failure time and the estimate of its expectation, while

"precision" is an expression of the spread (e.g., standard deviation). These indicators should also consider the fact that both the *RUL* and $E_t\{RUL\}$ (estimate, at time *t*, of the expectation of the equipment RUL) are random variables. Moreover, it is desirable that all indicators assume that, at any time *t*, it is possible to compute an estimate of the 95% confidence interval (CI_t) for the EOL.

In particular this paper uses three indicators to evaluate prognostic results, which are presented and detailed in (Orchard, Tobar and Vachtsevanos, 2009): (1) RUL precision index (RUL-OPI), (2) RUL accuracy-precision index, and (3) RUL online steadiness index (RUL-OSI). RUL-OPI considers the relative length of the 95% confidence interval computed at time *t* (CI_t), when compared to the RUL estimate. It is expected that the more data the algorithm processes, the more precise the prognostic becomes:

$$\text{RUL-OPI}(t) = e^{-\left(\frac{\sup(CI_t)-\inf(CI_t)}{E_t\{EOL\}-t}\right)} \qquad (9)$$
$$0 < \text{RUL-OPI}(t) \le 1, \forall t \in [1, E_t\{EOL\}), t \in \mathbb{N}.$$

The RUL accuracy-precision index, measures the error in EOL estimates relative to the width of its 95% confidence interval (CI_t). It also penalizes late predictions, i.e., whenever $E_t\{\text{EOL}\}$ (the expected EOL) is bigger than *GroundTruth*{EOL} (actual failure happens before the expected time). This indicator can be computed only after the end of the simulation. Finally, the RUL-OSI considers the variance of the EOL conditional expectation, computed with measurement data available at time *t*. Good prognostic results are associated to small values for the RUL-OSI. All performance metrics will be evaluated at all time instants.

In the case study presented in this paper (RUL/EOL estimation of a Li-Ion battery) the time is measured in cycles of operation. A cycle of operation consists of two different operational states applied to the battery at room temperature (charge and discharge).

It is essential to note that algorithm assessment only considered RUL estimates generated until the 120th cycle of operation, which corresponded to about 75% of the actual useful life of the battery (actual EOL of the experiment is 159 cycles), since it is of more interest to evaluate the algorithm's performance when the size of the prediction window is large enough to allow for corrective actions. Moreover, given that PF-based prognostic algorithms tend to improve their performance as the amount of available data increases (Orchard and Vachtsevanos, 2009), the closer the system is to the actual EOL, the more accurate the resulting EOL estimate. This needs to be kept in mind when analyzing results presented both in Figure 1 and Figure 2.

Figure 1 (a) shows online tracking for the battery SOH (coarse trace) using a classic PF-based prognostic approach until the 120th cycle of operation, the hazard zone around 1.2 [A-hr] (marked as a horizontal band), and the 95% confidence interval of EOL (coarse vertical dashed lines) computed at the 120th cycle. Figure 1 (b) only shows the EOL pdf estimate computed at the end of the 120th cycle of operation. The result of the classic PF-based prognostic approach is accurate to two cycles (the expected value of the EOL pdf is 161 cycles, while the ground truth data for the EOL is 159 cycles). However, the state estimate, in this case, does not exhibit the same level of accuracy when describing capacity regeneration phenomena registered at the 19th, 30th, and 47th cycles of operation; see Table 1. In fact, regeneration phenomena momentarily affect the algorithm performance, in particular in terms of steadiness of the solution (Orchard, Tobar and Vachtsevanos, 2009) as the analysis based on performance metrics will corroborate shortly.

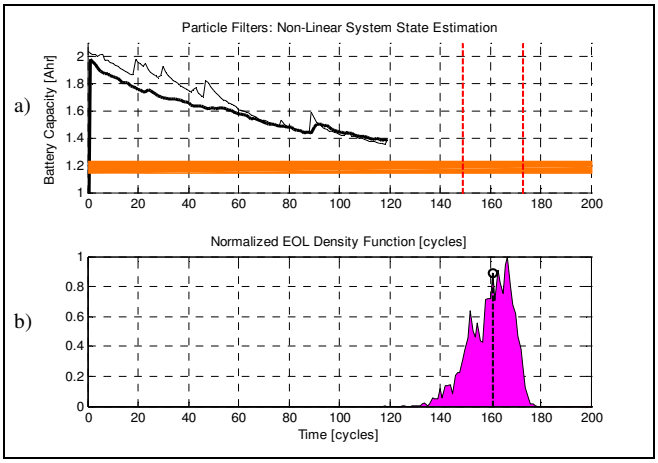

Figure 1. Case study. (a) Measurement data (fine trace), PF-based estimate (coarse trace), and 95% confidence interval (vertical read dashed lines). (b) EOL pdf estimate using classic PF-based prognosis framework and its expectation

Table 1. Estimates for system output $y(t)$

Cycle	Measured data	$E_t\{y(t)\}$ Classic PF-based routine	$E_t\{y(t)\}$ PF-based Anomaly detection and prognosis scheme
19th	1.98	1.77	1.80
30th	1.92	1.70	1.78
47th	1.82	1.62	1.69

Figure 2 (a) shows online tracking for the battery SOH (coarse trace) using the proposed scheme that combines a PF-based anomaly detection module to identify regeneration phenomena and a PF-based prognosis framework for the estimation of the battery EOL. This figure also illustrates the hazard zone around 1.2 [A-hr], and the 95% confidence interval of EOL computed at the 120th cycle. Figure 2 (b)

shows the EOL pdf estimate computed at the end of the 120th cycle of operation.

Figure 2 shows that the proposed scheme is equally capable of providing an accurate estimate of the battery RUL with an expected value of the EOL pdf (computed at the 120th cycle of operation) of 158 cycles, while the ground truth data for the EOL is 159 cycles). However, it is more interesting to note that the information provided by the anomaly detection module noticeably improves the state estimate at early stages of the test, particularly between the 20th and the 60th cycle of operation (see Table 1), allowing a better description of the regeneration phenomena that affect the Li-Ion battery. This demonstrates how the existence of particles in areas of low likelihood can help to improve the state estimate when rare, unlikely events or highly non-monotonic phenomena occur.

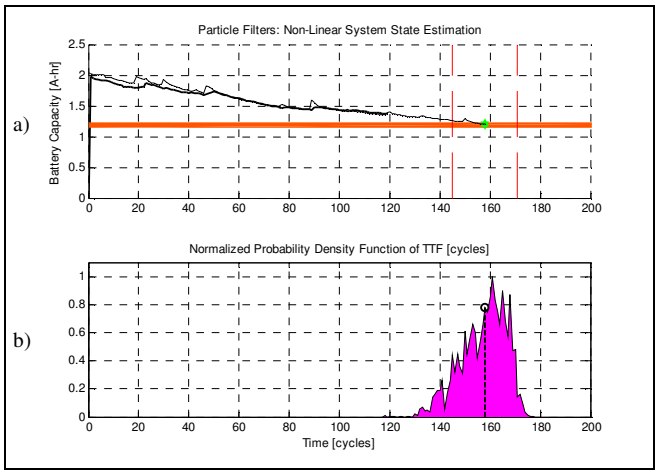

Figure 2. (a) Measurement data (fine trace), PF-based estimate (coarse trace), and 95% confidence interval. (b) EOL pdf estimate, using a combination of PF-based anomaly detection and prognosis approaches, and its expectation

Even more compelling, similar conclusions can be drawn when using prognostic performance metrics to assess the performance of the classic PF and the proposed scheme that includes an anomaly detection module; Figure 3 summarizes tracking and prediction with all tracking estimates generated until the 120th cycle.

Figure 3 (a) shows the evaluation of RUL-OPI as measurement data are included in a sequential manner into the prediction algorithm. One of the main characteristics of this indicator is that it penalizes the width of the 95th% confidence interval as the system approaches EOL. The value of this indicator is comparable for both algorithms (around 0.5 near the end of the experiment).

However, both the accuracy-precision and the RUL-OSI indices indicate noticeable advantages of the combination of PF-based anomaly detection and prognosis routines when compared to its classic version as illustrated in Figure 3 (b) and Figure 3 (c). The evaluation of the accuracy-precision index clearly shows improved performance in the case of the proposed framework, which translates into better estimates for the EOL conditional expectation. Similar conclusions can be obtained from Figure 3 (c), where the steadiness RUL-OSI index shows that the impact of detecting regenerating phenomena (and adjusting state estimates accordingly) is limited to bounded periods of time.

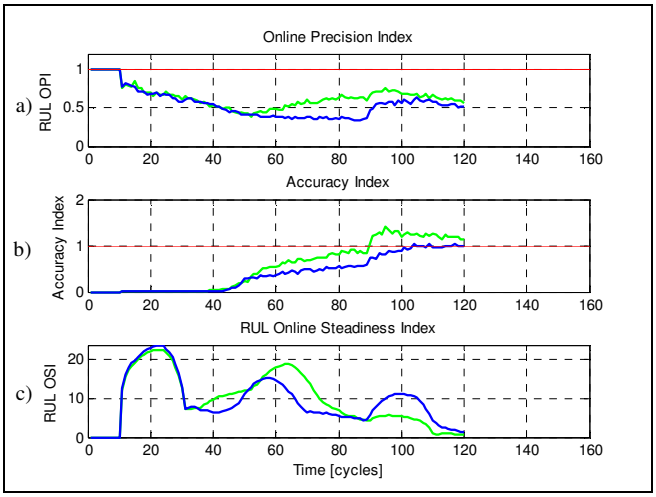

Figure 3. Performance metric evaluation in case study. Comparison between classic PF (green trace) and a combined PF-based anomaly detection/prognostic module (blue trace)

Previous research work (Orchard, 2009; Orchard and Vachtsevanos, 2009) has already shown better results when using classic PF-based prognostic framework, compared to other approaches. For this reason, this performance analysis did not consider other methods such as the extended Kalman filter in its formulation.

5. CONCLUSION

This paper presents a case study where a combined version of PF-based anomaly detection and classic PF-based prognosis algorithms is applied to estimate the remaining useful life of an energy storage device (Li-Ion battery). A comparison based on prognosis performance metrics indicates that the proposed anomaly detection/prognostic approach is more suitable than classic PF methods to represent highly non-monotonic phenomena such as capacity regeneration phenomena between charging periods, in terms of accuracy of the state estimate and steadiness of the RUL estimate. We surmise that the information provided by the anomaly detection module, in an online fashion, allow providing a more conservative estimate of the RUL of the faulty piece of equipment. We surmise that it also helps to incorporate the probability of rare and costly events in the evolution of the fault condition in time.

ACKNOWLEDGEMENT

The authors would like to acknowledge the support of NASA Aviation Safety Program/IVHM Project NRA NNA08BC20C. Thanks also go to Conicyt for Dr. Orchard's financial support via Fondecyt #1110070.

REFERENCES

Andrieu, C., A. Doucet, E. Punskaya, (2001). "Sequential Monte Carlo Methods for Optimal Filtering," in *Sequential Monte Carlo Methods in Practice*, A. Doucet, N. de Freitas, and N. Gordon, Eds. NY: Springer-Verlag.

Arulampalam, M.S., S. Maskell, N. Gordon, T. Clapp, (2002). "A Tutorial on Particle Filters for Online Nonlinear/Non-Gaussian Bayesian Tracking," *IEEE Transactions on Signal Processing*, vol. 50, no. 2, pp. 174 – 188.

Doucet, A., (1998). "On sequential Monte Carlo methods for Bayesian Filtering," Technical Report, Engineering Department, Univ. Cambridge, UK.

Doucet, A., N. de Freitas, N. Gordon, (2001). "An introduction to Sequential Monte Carlo methods," in *Sequential Monte Carlo Methods in Practice*, A. Doucet, N. de Freitas, and N. Gordon, Eds. NY: Springer-Verlag.

Orchard, M., G. Kacprzynski, K. Goebel, B. Saha, G. Vachtsevanos, (2008). "Advances in Uncertainty Representation and Management for Particle Filtering Applied to Prognostics," 2008 *International Conference on Prognostics and Health Management* PHM 2008, Denver, CO, USA.

Orchard, M., (2009). *On-line Fault Diagnosis and Failure Prognosis Using Particle Filters. Theoretical Framework and Case Studies*, Publisher: VDM Verlag Dr. Müller Aktiengesellschaft & Co. KG, Saarbrücken, Germany, 108 pages. Atlanta: The Georgia Institute of Technology, Diss., 2007.

Orchard, M. G. Vachtsevanos, (2009). "A Particle Filtering Approach for On-Line Fault Diagnosis and Failure Prognosis," Transactions of the Institute of Measurement and Control, vol. 31, no. 3-4, pp. 221-246.

Orchard, M., F. Tobar, G. Vachtsevanos, (2009). "Outer Feedback Correction Loops in Particle Filtering-based Prognostic Algorithms: Statistical Performance Comparison," *Studies in Informatics and Control*, vol.18, Issue 4, pp. 295-304.

Orchard, M., L. Tang, K. Goebel, G. Vachtsevanos, (2009). "A Novel RSPF Approach to Prediction of High-Risk, Low-Probability Failure Events," First Annual Conference of the Prognostics and Health Management Society, San Diego, CA, USA.

Patrick, R., M. Orchard, B. Zhang, M. Koelemay, G. Kacprzynski, A. Ferri, G. Vachtsevanos, (2007). "*An Integrated Approach to Helicopter Planetary Gear Fault Diagnosis and Failure Prognosis*," 42nd Annual Systems Readiness Technology Conference, AUTOTESTCON 2007, Baltimore, USA.

Verma, V., G. Gordon, R. Simmons, S. Thrun, (2004). "Particle Filters for Rover Fault Diagnosis," *IEEE Robotics & Automation Magazine*, pp. 56 – 64.

Vachtsevanos, G., F.L. Lewis, M.J. Roemer, A. Hess, B. Wu, (2006). *Intelligent Fault Diagnosis and Prognosis for Engineering Systems*, Hoboken, NJ, John Wiley and Sons.

Zhang, B., T. Khawaja, R. Patrick, M. Orchard, A. Saxena, G. Vachtsevanos, (2009). "A Novel Blind Deconvolution De-Noising Scheme in Failure Prognosis," *IEEE Transactions on Instrumentation and Measurement*, vol. 58, no. 2, pp. 303-310.